

Dataset Bias in Few-shot Image Recognition

Shuqiang Jiang, *Senior Member, IEEE*, Yaohui Zhu, Chenlong Liu,
Xinhang Song, Xiangyang Li, and Weiqing Min

Abstract—The goal of few-shot image recognition (FSIR) is to identify novel categories with a small number of annotated samples by exploiting transferable knowledge from training data (base categories). Most current studies assume that the transferable knowledge can be well used to identify novel categories. However, such transferable capability may be impacted by the dataset bias, and this problem has rarely been investigated before. Besides, most of few-shot learning methods are biased to different datasets, which is also an important issue that needs to be investigated in depth. In this paper, we first investigate the impact of transferable capabilities learned from distributions of base categories. Specifically, we introduce relevance to describe relationships of base and novel categories, along with instance diversity and category diversity to depict distributions of base categories. The FSIR model learns better transferable knowledge from relative training data. In the relative data, diverse instances or diverse categories can further enrich the learned knowledge. We conduct experiments on different sub-datasets of ImagNet, and experimental results demonstrate category relevance and category/instance diversity can depict transferable bias from distributions of base categories. Second, we investigate performance differences on different datasets from dataset structures and different few-shot learning methods. Specifically, we introduce image complexity, inner-concept visual consistency, and inter-concept visual similarity to quantify characteristics of dataset structures. We conduct comprehensive experiments on five different datasets (i.e., miniCharacter, minilmageNet, miniPlaces, miniFlower, miniFood) with four few-shot learning methods. We use these quantitative characteristics and few-shot learning methods to analyze performance differences on different datasets. Based on experimental analysis, some insightful observations are obtained from the perspective of both dataset structures and few-shot learning methods. These observations are useful to guide future few-shot learning research on new datasets or tasks.

Index Terms—Few-shot image recognition, meta learning, knowledge transfer, dataset bias

1 INTRODUCTION

LEARNING from few examples and generalizing to different situations are capabilities of human visual intelligence. During the past years, significant progress has been made on image recognition [1], [2], [3] with the assistance of deep learning techniques [4] and large scale labelled dataset [5], [6], however, this kind of human visual intelligence is yet to be matched by leading machine learning models. Humans can easily learn to recognize a novel object category after glancing only one or a few examples [7]. This cognitive ability can be explained by the "learning to learn" mechanism in the brain [8], which means that human can make inference so that their previously acquired knowledge on related tasks can be flexibly adapted to a new task. Inspired by this human ability, the few-shot image recognition (FSIR) is proposed to learn novel concepts from a few, or even a single example.

The task of FSIR establishes a new recognition setup to transfer the knowledge of training tasks sampled from training (base) categories to the new task with one or very few samples available. Instead of learning one single recognition task, most FSIR models learn plenty of recognition tasks. Each task contains a support set (training samples) and a target set (test samples). The support set consists of a few available labelled data, which is exploited to learn a

task-specific model. Then the learned model is evaluated on the target set. Each task in these two sets shares the same concepts. But concepts of testing tasks come from novel categories, which are different from those of training tasks.

Current studies of FSIR [9], [10], [11], [12], [13], [14], [15] achieve transferable knowledge by learning training tasks or base categories. These studies mostly focus on transferable knowledge between datasets or tasks by exploiting given base categories. The vast majority of current works assume the transferable knowledge to be globally shared across all tasks, and consider that the learned knowledge can be well adapted to novel categories. However, that transferable knowledge is highly dependent on distributions of base categories. FSIR models can acquire biased transferable capabilities if distributions of base categories and novel categories are very different. Furthermore, current studies rarely explore the characteristics of dataset structures, which include not only amount of information in the image but also semantic gaps between original images and concepts. Current works do not deeply dig differences in dataset structures. As a result, current few-shot learning methods might be biased to different datasets.

Two problems arise based on the above analysis: i) What factors can describe transferable bias from distributions of base categories? ii) What characteristics can depict bias of few-shot learning methods on different datasets? In this paper, we focus on studying these two problems systematically, which have rarely been explored before.

For the first problem, we aim to obtain knowledge from distributions of base categories, which can be better adapted to novel categories. The FSIR model can learn more

• The authors are with the Key Laboratory of Intelligent Information Processing of Chinese Academy of Sciences (CAS), Institute of Computing Technology, CAS, Beijing 100190, China and also with the University of Chinese Academy of Sciences, Beijing 100049, China.
E-mail: sqjiang@ict.ac.cn, {yaohui.zhu, chenlong.liu, xinhang.song, xiangyang.li}@vipl.ict.ac.cn, minweiqing@ict.ac.cn.

accurate knowledge from diverse instances, more comprehensive knowledge from diverse categories, particularly, transferable capabilities from relative categories. Therefore, we introduce dataset diversity to depict the distributions of base categories and relevance to describe relationships of base categories and novel categories. The dataset diversity contains instance diversity and category diversity. We conduct experiments on different sub-datasets of ImageNet [16] which contain diverse categories and diverse instances. We measure relationships of categories with the tree structure in ImageNet. Specifically, under the settings of relevance or irrelevance of base categories and novel categories, we explore instance diversity and category diversity, respectively. Besides, we further compare instance diversity and category diversity with the fixed number of total samples.

For the second problem, we aim to analyze differences in performance on different datasets from characteristics of dataset structures and different few-shot learning methods. We introduce image complexity, inner-concept visual consistency, and inter-concept visual similarity to quantify characteristics of dataset structures. To conduct comprehensive evaluation on multiple datasets, we introduce five datasets, including simple character images (i.e., miniCharacter), images with different number of objects (i.e., miniImagenet, miniPlaces), and two fine-grained datasets (i.e., miniFlower and miniFood). We use three kinds of features to calculate inner-concept visual consistency and inter-concept visual similarity, and measure image complexity in two manners. We use these quantitative characteristics to analyze differences in performance on different datasets. In addition, we give analysis on differences in performance with different few-shot learning methods.

In summary, our main contributions are as follows: i) We systematically investigate the influence of knowledge learned from base categories. ii) We systematically investigate differences in performance on different datasets with three characteristics of dataset structures and two types of few-shot learning methods. iii) Based on the above investigates, we can obtain following key conclusions:

- The FSIR model can obtain better performances with knowledge learned on relevant base categories rather than irrelevant ones.
- The FSIR model can obtain improvements with knowledge learned on more diverse instances or categories without reducing the relevance.
- The FSIR model can obtain more improvements with knowledge learned on diverse categories than that learned on diverse instances without reducing the relevance, when there are enough diverse instances for each category.
- The FSIR model obtain different performances on different datasets, which can be depicted with image complexity, inner-concept visual consistency, and inter-concept visual similarity.
- The metric-based method is suitable for datasets of simple visual patterns, while the meta-learning method can be explored for datasets of complex ones.

The reminder of this paper is constructed as follows. Section 2 provides the related work, including FSIR, domain adaptation, and few-shot domain adaptation. Section 3 gives

formulation of FSIR and reviews two types of classic few-shot learning methods. Section 4 presents evaluations of the dataset diversity in detail. Section 5 presents evaluations of the dataset structure and experimental analysis in detail. Finally, the paper closes with conclusions in Section 6.

2 RELATED WORK

2.1 Few-shot Image Recognition

The goal of FSIR is to identify novel categories with a few annotated examples and knowledge obtained from base categories. As an early attempt, Fei-Fei *et al.* [17] propose a variational bayesian framework for one-shot image classification, and Lake *et al.* [18] propose hierarchical bayesian program learning on the few-shot alphabet recognition tasks. Inspired by architectures with augmented memory capacities such as Neural Turing Machines (NTMs), Santoro *et al.* [19] propose a meta-learning method with memory-augmented neural networks. Afterwards, there are three kinds of methods to deal with the FSIR problem. The first one is metric-based method (i.e., learning to compare), which learns a transferable embedding network or function. This function transforms the original images into the embedding space such that these images can be recognized with a nearest neighbor [20], a linear classifier [9], [21] or a deep nonlinear metric [10]. The second one is meta-learning method [22], [23] (i.e., learning to learn), whose learning occurs at two levels: task-level learning and take-specific adaption. The task-level learning is usually implemented by an additional meta-learner [14], [24] or a sensitive initialization shared with task-specific learners [13], which can provide meta-level information for the take-specific adaption. The third method is generative or augmentation-based method (i.e., learning to generate or augment), which learns a generative model to synthesize more samples and then trains a robust classifier. This generative model uses semantic information [25], [26] (e.g., attribute), or base categories used for analogy or hallucination [27], [28].

Recently, some works study FSIR from the view of self-supervised approaches [29], [30] and semi-supervised approaches [31], [32]. Yu *et al.* [33] propose a two-stage approach which explores knowledge from both annotated examples of base categories and un-annotated ones of novel categories. The above works focus on learning transferable knowledge with given datasets. However, we investigate the performance of FSIR from dataset diversity with changeable base categories and different characteristics of dataset structures. A more related work is [34], which shows that increasing relevant categories in close or far semantic distances can boost the performance of FSIR. In addition, our work also considers increasing irrelevant categories, and experimental results illustrate that more irrelevant categories cannot improve the performance, suggesting that it's not the more categories the better performances. Furthermore, we investigate differences in performance on different datasets from the dataset structure and different few-shot learning methods, which is not explored by [34]. Therefore, we do different explorations from the work [34].

2.2 Domain Adaptation

Domain adaptation utilizes labeled data in one or more relevant source domains to execute new tasks in a target domain with scarce annotated data. It aims to solve the domain gap and transfer knowledge learned on the source domain to the target domain [35], [36], [37], [38]. As many approaches are based on deep neural networks, Li *et al.* [39] construct source and target datasets with various distances to analyze factors that affect the effectiveness of using prior knowledge from a pre-trained model with a fixed network architecture. Azizpour *et al.* [40] investigate factors (e.g., network architectures, parameters of feature extraction) affecting the transferability of feature representations in generic convolutional networks. To learn domain invariant features minimizing the domain discrepancy, Long *et al.* [41] propose a deep network architecture that can jointly learn adaptive classifiers and transferable features from labeled data in the source domain and unlabeled data in the target domain. Meanwhile, with significant advances made in image synthesis by generative adversarial networks, many methods focus on learning domain-independent features and synthesizing examples in the new domain [42], [43]. Hoffman *et al.* [44] propose adversarial learning method that utilizes both generative image space alignment and latent representation space alignment. Zhang *et al.* [45] propose an adversarial learning method with two-level domain confusion losses. Cui *et al.* [46] propose gradually vanishing bridge mechanism to learn more domain-invariant representations. To tackle predictive domain adaptation, Mancini *et al.* [47] leverage metadata information to build a graph and design novel domain-alignment layers based on the graph for domain adaption. These works have the same classes among different domains. In contrast, we address the problem that the classes in target domain are different from the ones of source domains and the examples in the target domain are limited or rare.

2.3 Few-shot Domain Adaptation

Few-shot domain adaptation aims to recognize novel categories with a few annotated data in the target domain and sufficient data in the source domains. Some works [48], [49] assume that the target domain contains the same classes as the source domain. Recently, some efforts attempt to address a more flexible and challenging few-shot domain adaptation, where the target domain and source domains have disjoint classes, called cross-domain few-shot learning. Chen *et al.* [11] evaluate current models and proposed baselines on cross-domain few-shot protocols (from miniImageNet [21] to cub [50]). Tseng *et al.* [51] propose a learned feature-wise transformation to stimulate feature distributions cross domains with a small number of samples. Guo *et al.* [52] introduce a more realistic cross-domain few-shot learning, where the source domain consists of common images from Imagenet [16], and the target domains contain rare images such as satellite images and radiological images. Besides, Vuorio *et al.* [53] propose the multi-domain few-shot learning, and use a task-aware modulation to promote the learning of meta learner. Yao *et al.* [54] propose a hierarchically structured meta-learning algorithm to promote knowledge

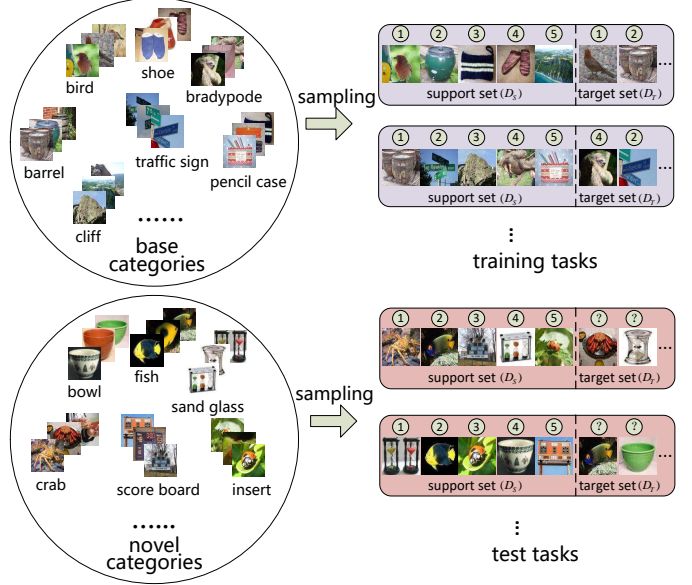


Fig. 1. The training and test tasks are formed by randomly sampling from the base and novel categories, respectively.

customization on different domains but simultaneously preserve knowledge generalization in related domains. Triantafillou *et al.* [55] introduce a meta-dataset that consists of 10 datasets in different domains and present experimental evaluation of current models and proposed baselines. These works only use given source domains without selections, in contrast, we selectively use source domains (i.e., base categories) and systematically investigate different target domains from characteristics of dataset structures and different few-shot learning methods.

3 PRELIMINARIES

3.1 Few-shot Image Recognition Formulation

In the regular machine learning setting, a classification problem is defined on instances $\mathcal{I}_{(x,y)} \sim p(\mathcal{I})$, where x is a sample and y is the corresponding label. But most FSIR models learn task instances $\mathcal{T} \sim p(\mathcal{T})$. Sampling from training and test data, we form training tasks \mathcal{T}^{train} and testing tasks \mathcal{T}^{test} , respectively. According to existing settings, the training and test data are made of base and novel categories, respectively, and each category has plenty of samples. For example, in miniImageNet [21], the number of base and novel categories are 64 and 20, respectively, where each category has 600 samples.

In training tasks \mathcal{T}^{train} or testing tasks \mathcal{T}^{test} , each task is defined as $\mathcal{T}_j = \{D_{\mathcal{T}_j,S}, D_{\mathcal{T}_j,T}\}$, where $D_{\mathcal{T}_j,S}$ is a support set (training samples) and $D_{\mathcal{T}_j,T}$ is a target set (test samples). The support set $D_{\mathcal{T}_j,S} = \{(x_c^k, y_c^k) \mid c = 1, 2, \dots, C; k = 1, 2, \dots, K\}$ and the target set $D_{\mathcal{T}_j,T}$ consist of C categories randomly sampled from the total categories, and each sampled category contains K labeled samples in the support and some samples in the target set. And this task is called C -way K -shot task. Test tasks \mathcal{T}^{test} and training tasks \mathcal{T}^{train} have the same form but with disjoint label space since they have different categories. Fig. 1 illustrates the 5-

way 1-shot training and test tasks, which are sampled from base and novel categories, respectively.

3.2 Few-shot Learning Methods

Metric-based methods and Meta-learning methods are employed to explore the dataset bias. These two kinds of methods do not use additional information and are easy to implement with less options, compared with generative or augmentation-based method. Hence, the current metric-based methods and meta-learning methods are fully utilized, and the corresponding typical works are introduced in the following.

3.2.1 Metric-based Methods

This kind of method contains two parts: an embedding network or function $\mathcal{G}()$ and a metric $\mathcal{M}()$. A key assumption is that $\mathcal{G}()$ learns domain-general information as an inductive bias [56] to generalize novel category. In addition, the learning target or the loss function $\mathcal{L}()$ affects $\mathcal{G}()$ learning (or $\mathcal{M}()$ learning, when $\mathcal{M}()$ is parameterized). Hence, we review the following metric-based few-shot learning methods from $\mathcal{L}()$ and $\mathcal{M}()$.

Prototypical Net (PN) [9]. In this method, the $\mathcal{M}()$ is the Euclidean distance. The $\mathcal{L}()$ is cross entropy loss, and the probability of each sample in D_T is defined as (omitting the index of task):

$$P(\bar{y}|\bar{x}, D_S) = \frac{e^{-\mathcal{M}(\mathcal{G}(\bar{x}), \sum_{(x,y) \in D_S} \frac{\mathbf{I}\{y=\bar{y}\}\mathcal{G}(x)}{K})}}{\sum_{a=1}^C e^{-\mathcal{M}(\mathcal{G}(\bar{x}), \sum_{(x,y) \in D_S} \frac{\mathbf{I}\{y=y_a\}\mathcal{G}(x)}{K})}} \quad (1)$$

Where C is the number of way and K is the number of shot.

Relation Network (RN) [10]. This method learns a parameterized $\mathcal{M}()$, which is implemented by a neural network. The $\mathcal{L}()$ is mean square error, defined as:

$$\sum_{(\bar{x}, \bar{y}) \in D_T} \sum_{(x, y) \in D_S} (r(\bar{y}|\bar{x}, D_S) - \mathbf{I}\{y = \bar{y}\})^2 \quad (2)$$

Where $r(\bar{y}|\bar{x}, D_S) = \mathcal{M}(\mathcal{G}(\bar{x}), \text{pooling}(\{\mathcal{G}(x) \mid (x, y) \in D_S, y = \bar{y}\}))$, and the $\text{pooling}()$ is maxpooling in [10].

3.2.2 Meta-learning Methods

This kind of method usually contains two parts: an initial model $\mathcal{F}(\cdot; \theta)$ and a rapid-adapted strategy $\mathcal{S}(\cdot; \delta)$, where θ are parameters of $\mathcal{F}()$, and δ are parameters of $\mathcal{S}()$. The processes of this kind of method are: i) computing the gradient (or loss) information on support set: $\mathbf{grad}_{a_t/\theta} = \nabla_{a_t/\theta} \mathcal{L}(\mathcal{F}(D_S(x); \theta), D_S(y))$, where $\mathcal{L}(\cdot)$ is the loss function, a_t is the t^{th} neurons of $\mathcal{F}()$; ii) transforming the gradient information into adaptive information: $I = \mathcal{S}(\mathbf{grad}; \delta)$; iii) leveraging the adaptive information to obtain adaptive model: $\mathcal{B}(\mathcal{F}(\cdot; \theta), I)$. Similarly, we review the following meta-learning methods from the $\mathcal{S}()$. Generally speaking, the final learning target or the loss function is the same with $\mathcal{L}()$, mentioned in the processes, calculated on the target set.

Model-Agnostic Meta-Learning (MAML) [13]. This method is inspired by fine-tuning. It computes gradient of the whole parameter θ , and then directly uses the gradient on original parameters with one or a few gradient steps

to obtain adaptive model: $\mathcal{B}(\mathcal{F}(\cdot; \theta), I) = \mathcal{F}(\cdot; \theta - rI)$, where $I = \mathbf{grad}_\theta$, r is updating learning rate.

adaCNN [14]. This method computes gradient of neurons $\mathbf{grad}_t = \nabla_{a_t} \mathcal{L}(\mathcal{F}(D_S(x); \theta), D_S(y))$, and transforms the gradient into conditional shift vectors $\beta_{t,m} = I_{m,t} = \mathcal{S}(\mathbf{grad}_{a_t,m}; \delta)$ (m is the m^{th} instance in the support set) that are saved in a memory. The adaptive model is as follows:

$$\mathcal{B}(\mathcal{F}(\cdot; \theta), \beta_t) = \begin{cases} \sigma(\mathcal{F}(a_t; \theta)) + \sigma(\beta_t) & t \neq T \\ \text{softmax}(\mathcal{F}(a_t; \theta) + \beta_t) & t = T \end{cases} \quad (3)$$

Where T is the final layer, $\sigma()$ is a nonlinear function and $\text{softmax}()$ is the Softmax function. The layer-wise shifts are recalled from memory via a soft attention to obtain β_t ($\beta_t = \sum_m w_m \beta_{t,m}$, w_m is calculated by a key function), which is used for adjusting the output of initial model.

3.2.3 Impacts of Data Distribution

Metric-based methods do not need task-specific adaptation. They require data with a high relevance between base categories and novel categories especially for a learnable metric. Metric-based methods may excel at recognizing novel categories of simple visual patterns but they may be confused to identify visually similar novel categories. Metric-based methods need the adaptation. They are less dependent on the relevance, compared with metric-based methods. Metric-based methods can identify similar categories with the adaptation, but this adaptation sometimes introduces noises. Thus, the two kinds of methods have respective characteristics to handle different data.

4 EVALUATION OF DATASET DIVERSITY

The FSIR model aims to recognize novel categories with a small amount of samples by exploiting learnable generic knowledge. This kind of knowledge is learned from sufficient base categories, whose diversity can explicitly affect the quality of the learned knowledge. In this section, we study dataset diversity of base categories to explore FSIR. First, we introduce some key factors of dataset diversity. Second, we present evaluated datasets and settings. Next, we explore these factors independently and compare them. Finally, we give some discussions.

4.1 Factors of Dataset Diversity

The dataset diversity can be reflected in two aspects including instance and category diversity. On one hand, diverse instances can provide each concept with lots of variations in pose, scale, illumination, distortion, background, etc. Thus the FSIR model can learn more accurate knowledge from diverse instances. On the other hand, diverse categories can provide plenty of concepts with big visual differences. Thus the FSIR model can learn more comprehensive knowledge from diverse categories.

4.2 Evaluated Datasets and Settings

As ImageNet [16] is a well-known large data set which has been widely used for both visual recognition and

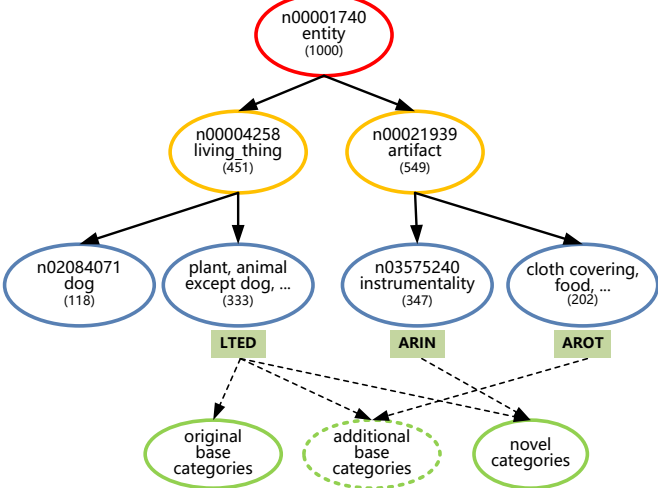


Fig. 2. The hierarchical display of the 1000 categories in ImageNet. The integer in the parenthesis indicates the number of the categories that the branch contains. The number in the beginning of the node is the corresponding WordNet ID. The LTED, ARIN and AROT are three branches, which are sampled to form original (additional) base and novel categories.

FSIR (e.g., miniImageNet [21]), we construct different sub-datasets which contain diverse categories and diverse instances for FSIR. We focus on the 1000 categories in ImageNet (ILSVRC2012), with 1.28 million images in total. For each category, it belongs to one synset in WordNet [57]. We find its parent synsets recursively until reaching the node of entity which is the root of the WordNet, according to their hierarchical semantic relations. In this manner, we can obtain the entire tree structure of the 1000 categories, which are divided into different branches with different relevances.

The divided branches of the 1000 categories are illustrated in Fig. 2. All categories belong to the entity branch, as the entity node is the root of the tree structure. And then, they are divided into two branches according to whether they are man-made or nature. More precisely, as shown in Fig. 2, the first one is living thing branch which contains 451 categories, and the second one is artifact branch which contains 549 categories. The living thing branch is continuously divided into the dog branch (which contains various dogs) and the LTED (which is the short for Living Thing Except Dog) branch which is the rest of the living thing branch except the categories in the dog branch. Meanwhile, the artifact branch is divided into the ARIN (which is short for ARTifact INstrument) branch which is the super class of instrumentality and the AROT (which is short for ARTifact Other Thing) branch which is the rest of the artifact branch.

To measure the relevance between different categories, we refer to the approaches utilized by [39], [58], and qualitatively estimate their relevance according to the tree structure of ImageNet. The categories in the same branch are more relevant than the ones in different branches. For example, categories in LTED contain animals such as cat, sheep, kangaroo, while categories in ARIN contain many traffic instruments. These animals in LTED are relevant to each other as they have eyes, legs and tails while objects (e.g., lock, fishing pole, and mouse) in ARIN do not have. The few-shot learning model would suffer from handling a sequence

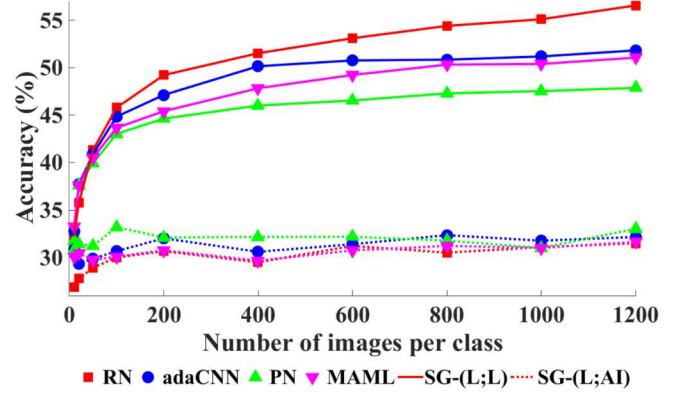


Fig. 3. 5-way 1-shot accuracy of SG-(L;L) and SG-(L;AI).

of training tasks originated from different distributions if the novel categories are irrelevant to the base categories. In this section, we do not use dog branch since this branch lacks of diversities of images. And then base and novel categories are sampled from the LTED, ARIN, and AROT branches to explore the dataset diversity for FSIR.

In the following sub-sections, we carry out various groups of experiments, which are based on different base and novel categories. A group of experiment includes original or with additional base categories and novel categories, as illustrated in Fig 2. Each group of experiments is conducted 5 times with four few-shot learning methods (i.e., PN [9], RN [10], MAML [13], adaCNN [14]) to obtain stable and reliable performance. The four methods use a 4 convolutional layers as meta-learner (backbone) with the different number of filters per layer. We adopt the architectures of corresponding methods without modification for our experiments. Without loss of generality, we analyze the factors of dataset diversity on 1-shot models. To evaluate each model, 400 test tasks are randomly sampled from 20 novel categories. And each test task has 5 classes, each of which has 1 image at the support set and 15 images at the target set. These test settings have been widely used in the few-shot evaluation [9], [10], [13], [14], [21], [24], and the results are reported with mean accuracy.

4.3 Instance Diversity

This subsection studies the problem of whether increasing the instances diversity can bring better performances on test tasks. Different from the study of the impact of the shot number [59], this subsection aims to investigate the impact of performance as the number of samples per base category increases. We conduct two groups of experiments with the samples growth (SG) per base category, and each of them uses 64 base categories with the number of samples per category ranging from 10 to 1200. One group uses base and novel categories sampled from LTED branch, denoted as SG-(L;L). Another group uses the same base categories, but it employs novel categories sampled from ARIN branch, denoted as SG-(L;AI). Each novel category in SG-(L;L) has more relevant base categories than that in SG-(L;AI). In other word, SG-(L;L) uses relevant base categories while SG-(L;AI) employs irrelevant ones.

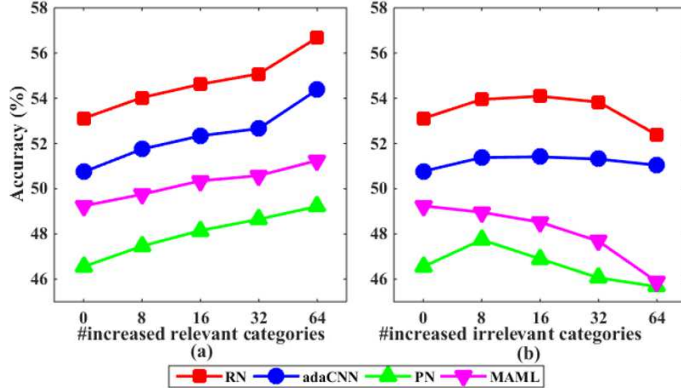


Fig. 4. (a) and (b) present the 5-way 1-shot accuracy of CG-(L,L;L) and CG-(L,AO;L), respectively.

Fig. 3 displays the performances of the two groups. It can be observed that: i) The performance of SG-(L;L) exceeds SG-(L;AI) by a wide margin with the same methods, especially as the number of samples per base category increases. ii) In SG-(L;L), more instances lead to better performance, and the performance improvement is fast when the number of samples per base category ranges from 10 to 200, while it gets slow when starting from 200. iii) In SG-(L;AI), the performance is improved at the beginning of the number of instances increasing (from 10 to 100), after which the performance is not significantly improved.

The following suggestions can be obtained.

- It is very important to use plenty of instances of relevant base categories to train the FSIR model.
- If the relevant base categories are not available, there is no need to use too much instances of each category.

4.4 Category Diversity

This subsection studies the problem of whether increasing the category diversity can bring better performances on test tasks. Since the number of base categories is changed, we divide base categories into original and additional ones. We set up two groups of experiments with category growth (CG), and each of them uses 64 original base categories and varying additional ones. One group employs original, additional base categories and novel categories all sampled from LTED branch, denoted as CG-(L,L;L). Another group exploits the same original base and novel categories, but it uses additional base categories sampled from AROT branch, denoted as CG-(L,AO;L). It is obvious that CG-(L,L;L) uses relevant additional base categories while CG-(L,AO;L) employs irrelevant ones. The number of samples per original or additional base category is 600. The samples of original base categories are fixed in the same group, and the number of additional base categories ranges from 0 to 64.

Experimental results of CG-(L,L;L) and CG-(L,AO;L) are illustrated in Fig. 4 (a) and (b), respectively. It can be observed that: i) When additional base categories are relevant to novel categories, more additional categories lead to better performances (see Fig. 4 (a)). ii) When additional base categories and novel categories are irrelevant, the performance may be improved at the beginning of the number

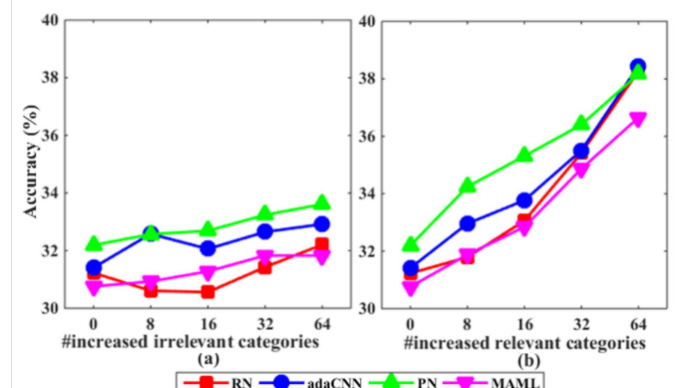


Fig. 5. (a) and (b) present the 5-way 1-shot accuracy of CG-(L,L;AI) and CG-(L,AO;AI), respectively.

TABLE 1
Sampled categories of different groups.

Groups	Base categories original	additional	Novel categories
SG-(L;L)	LTED	-	LTED
SG-(L;AI)	LTED	-	ARIN
CG-(L,L;L)	LTED	LTED	LTED
CG-(L,AO;L)	LTED	AROT	LTED
CG-(L,L;AI)	LTED	LTED	ARIN
CG-(L,AO;AI)	LTED	AROT	ARIN
CGS-(L,L;L)	LTED	LTED	LTED
CGS-(L,L;AI)	LTED	LTED	ARIN
CGS-(L,AO;L)	LTED	AROT	LTED
CGS-(L,AO;AI)	LTED	AROT	ARIN

of categories increasing, after which the performance drops (see Fig. 4 (b)).

On the other hand, we set another two groups of experiments denoted as CG-(L,L;AI) and CG-(L,AO;AI). Different from the above two groups, novel categories of them are sampled from ARIN branch, as illustrated in Table 1. Obviously, CG-(L,L;AI) uses irrelevant additional base categories while CG-(L,AO;AI) employs relevant ones.

Experimental results of CG-(L,L;AI) and CG-(L,AO;AI) are illustrated in Fig. 5 (a) and (b), respectively. It can be observed that: i) The performance of CG-(L,AO;AI) is obviously superior to CG-(L,L;AI) as the number of additional base categories increases. The main reason is that CG-(L,AO;AI) uses relevant additional base categories while CG-(L,L;AI) uses irrelevant ones. ii) The performances of two groups are improved as the number of additional base categories increases. In addition, comparing CG-(L,L;L) and CG-(L,AO;AI) (or CG-(L,AO;L) and CG-(L,L;AI)), relevant original base categories provide a better initial performance than irrelevant ones.

The following suggestions can be obtained.

- It is very important to use plenty of relevant base categories to learn the FSIR model.
- If original base categories are not relevant to novel categories, we can use some additional base categories without constraints.

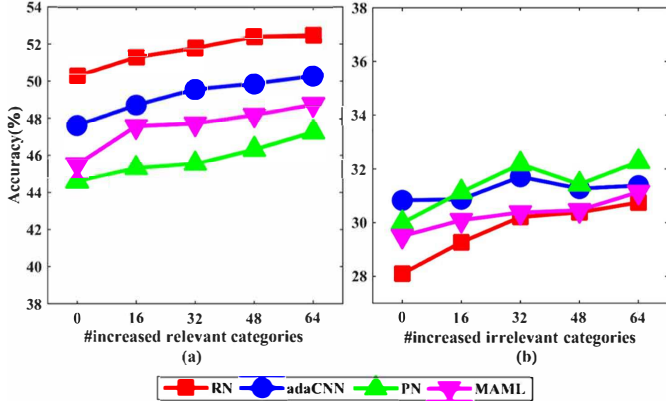


Fig. 6. (a) and (b) present the 5-way 1-shot accuracy of CGS-(L,L;L) and CGS-(L,L;AI), respectively.

4.5 Instance Diversity v.s. Category Diversity

From the above experiments, the FSIR performance would be improved by increasing relevant instances or relevant categories of base categories. To further explore which factor is more effective to boost the performance, we make comparisons by fixing the number of total samples while varying the number of categories and the number of samples in each categories. In this case, the number of samples in each category will be decreased to guarantee the same total number of samples, as the number of base categories increases. Since the relevance of base and novel categories would affect the performance, we set up two groups of experiments with the same relevance of original and additional base categories, and each of them includes 32 original base categories and varying additional ones. One group employs categories all sampled from LTED branch, denoted as CGS-(L,L;L) (Category Growth under the Same total samples). Another group exploits the same original and additional base categories, but it uses novel categories sampled from ARIN branch, denoted as CGS-(L,L;AI). Thus CGS-(L,L;L) uses relevant base categories while CGS-(L,L;AI) employs irrelevant ones. Original base categories are fixed in the same group of experiments, and the number of additional base categories ranges from 0 to 64. The total number of samples of base categories is 38400 (equal to the number of total training samples in miniImageNet), where each base category contains equal number of samples. Since the total number of samples of base categories is fixed, each original base category would have less samples with the growth of the number of additional base categories. For example, each original base category contains 1200 samples without additional base categories (the total number is $1200 \times 32 = 38400$), and the number of samples of each original base category would reduce to 800 when 16 additional base categories with 800 samples per category are used (the total number is $800 \times (32+16) = 38400$).

Experimental results of CGS-(L,L;L) and CGS-(L,L;AI) are illustrated in Fig. 6 (a) and (b), respectively. It can be observed that increasing base categories is more effective than increasing their samples to boost the FSIR performance, when original and additional base categories are relevant. This is to say, it is better for the FSIR model to use more relevant base categories than more samples per relevant

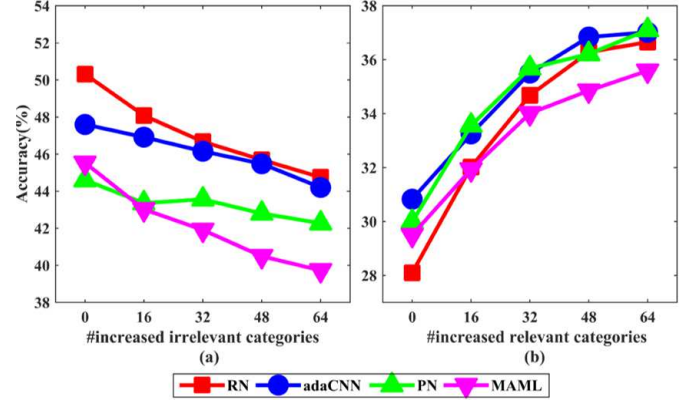


Fig. 7. (a) and (b) present the 5-way 1-shot accuracy of CGS-(L,AO;L) and CGS-(L,AO;AI), respectively.

base category (obtained from Fig. 6 (a)), and it is better for the FSIR model to use more irrelevant base categories than more samples per irrelevant base category (obtained from Fig. 6 (b)). This phenomenon explain that additional base categories provide more bonus for the FSIR model than learned categories with additional samples, since the model has already learned accurate knowledge from hundreds of samples per base category.

Moreover, we set another two groups of experiments with irrelevance of original and additional base categories. The two groups are denoted as CGS-(L,AO;L) and CGS-(L,AO;AI), which are different from the above two groups since they use additional base categories sampled from AROT branch, as illustrated in Table 1. Obviously, CGS-(L,AO;L) uses irrelevant additional base categories while CGS-(L,AO;AI) employs relevant additional ones, and CGS-(L,AO;L) uses relevant original base categories while CGS-(L,AO;AI) employs irrelevant original ones.

Experimental results of CGS-(L,AO;L) and CGS-(L,AO;AI) are illustrated in Fig. 7 (a) and (b), respectively. From Fig. 7 (a), it is better for the FSIR model to use more samples per relevant base category than more irrelevant base categories. From Fig. 7 (b), it is better for the few-shot recognition to use more relevant base categories than more samples per irrelevant base category. These two observations can explain that relevance is a more important factor than more base categories or more sample per base category.

The following suggestions can be obtained.

- It is better for the FSIR model to use more base categories than more samples per category, when original and additional base categories are relevant.
- Relevance is a more important factor than transformations in sample forms (i.e., more categories or more sample per category).

According to the above two points, we can further infer that the FSIR performance goes down in order of more relevant base categories, more samples per relevant base category, more irrelevant base categories, and more samples per irrelevant base category.

4.6 Tremendous Number of Categories

When the number of total samples is fixed, whether more base categories lead to better the FSIR performance? To

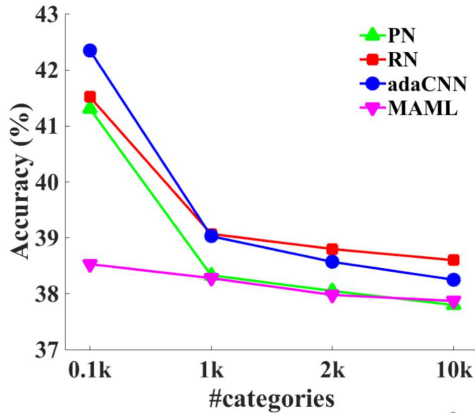


Fig. 8. Experimental results on a large number of categories with a fixed amount of total samples.

explore this problem, we conduct experiments on a dataset of a larger number of categories. This dataset contains 10,020 categories, sampled from ImageNet [16]. In this case, we set the total number of samples as 20,000, and the number of base categories ranges from 100 to 10,000, thus, each category contains samples ranging from 200 to 2. For each setting (indexed with the number of base categories), the evaluations are also conducted 5 times with four few-shot learning methods. Evaluating each model, we use the same architecture of few-shot learning methods, the same number of test tasks or novel categories, and evaluation index as the above experiments.

Experimental results are illustrated in Fig. 8. With the fixed number of total samples, as the number of base categories increases, the FSIR performance decreases. When the number of per base category is 1000, namely each base category contains 20 samples, more samples per base category become more important than more base categories. In this case, additional samples per base category provide more bonus for the FSIR model than additional base categories, since the FSIR model can not learn accurate knowledge well from a small amount of samples per category.

4.7 Discussion

The main factors about base categories affecting the performance of FSIR are presented as follows.

- The more categories is not always the better. Relevance is the key factor, increasing relevant categories can benefit FSIR, otherwise, including irrelevant categories may not be helpful.
- Data diversity is also an important factor to FSIR, large diversity in categories or instances can result in better results, since diversity in training data may enhance the generalization capability.
- When enough instance diversity is in each category, category diversity is more sensitive than instance diversity, which may coarsely broaden the diversity of whole dataset, meanwhile, enhancing the generalization capability of the FSIR model.



Fig. 9. The rank of some examples on image complexity. Simple images are in the bottom, and more complex image is in a higher position.

5 EVALUATION OF DATASET STRUCTURE

As the early studies, FSIR attempts to recognize the alphabet [18] and images with simple background [17]. Afterwards, FSIR focuses on more realistic images such as general object images [9], [10], [21], [27], fine-grained object images [21], [60], scene images [25], [28]. Different datasets present different difficulty levels of FSIR. For example, FSIR on alphabet images is easier than that on real-world images. This reflects the differences of intrinsic dataset structures on different datasets. In this section, we study the dataset structure from the view of FSIR. First, we present various factors of dataset structures with quantitative representations. Second, we introduce several datasets under few-shot settings. And then we make analysis on different datasets from the dataset structure and few-shot learning methods. Finally, we give some discussions.

5.1 Factors of Dataset Structure

Dataset structure can be reflected with image complexity and inner-concept visual consistency, inter-concept visual similarity. Image complexity can depict visual contents of original images. If original images include complex background information, it could be difficult to accurately identify their concepts. As illustrated in Fig. 9, the apple image is more complex than the letter "L" image, and the scene image is more complex than the apple image. Both inner-concept visual consistency and inter-concept visual similarity can depict semantic gaps between low-level visual features (i.e., computational representations of images from hand-crafted algorithms) and high-level image concepts (i.e., semantic interpretations of images from human beings) [61]. Inner-concept visual consistency describes the aggregations of single concept in the visual feature space, and a big inner-concept visual consistency may result in low semantic gaps. In contrast, inter-concept visual similarity describes correlations between different concepts in the visual feature space,

and a small inter-concept visual similarity may result in low semantic gaps.

We quantify image complexity with the following ways: i) Complex images often have complex structures, and structural attributes can be preserved by edges. We use percentage of edge points P_{EP} as a metric, defined as:

$$P_{EP} = \frac{\#(\text{edge pixels})}{\#(\text{image pixels})} \quad (4)$$

where $\#(\text{image pixels})$ and $\#(\text{edge pixels})$ are the number of pixels and edges in the image, respectively. Edge pixels can be detected with the Canny edge detection method [62]. ii) We utilize the 2D entropy E_{2D} [63] to measure the underlying spatial structure and pixel co-occurrence. Given an $N \times M$ pixel image $f(n, m)$, E_{2D} is defined as:

$$E_{2D} = - \sum_{i=I_{min}}^{I_{max}} \sum_{j=J_{min}}^{J_{max}} p_{i,j} \log_2 p_{i,j} \quad (5)$$

where $p_{i,j} = \frac{1}{N \times M} \sum_{n=1}^N \sum_{m=1}^M \delta_{i,f_x(n,m)} \delta_{j,f_y(n,m)}$, δ is the Kronecker delta formulation, f_x and f_y are the two derivative components of the gradient field, I and J record all gradient values in two gradient directions.

Inner-concept visual consistency and inter-concept visual similarity are quantified according to [61]. Inner-concept visual consistency of category C_l is defined as: $c_{inn}(C_l) = \frac{2}{|C_l| * (|C_l| - 1)} \sum_{i=1}^{|C_l|} \sum_{j=i+1}^{|C_l|} k(x_l^i, x_l^j)$, where $|C_l|$ is the number of images in C_l , x_l^i and x_l^j are the feature representations of images in C_l , $k(x_l^i, x_l^j) = c / \sqrt{|x_l^i - x_l^j|^2 + c}$ (c is a scalar, $k(x_l^i, x_k^j)$ is inversely proportional to the Euclidean distance of x_l^i and x_k^j , and can be used as the similarity of them). The average inner-concept visual consistency C_{inn} of all categories in D is defined as:

$$C_{inn} = \frac{1}{|D|} \sum_{l=1}^{|D|} c_{inn}(C_l) \quad (6)$$

where $|D|$ is the number of categories in D . Inter-concept visual similarity between C_l and C_k is defined as: $s_{int}(C_l, C_k) = \frac{1}{|C_l| |C_k|} \sum_{i=1}^{|C_l|} \sum_{j=1}^{|C_k|} k(x_l^i, x_k^j)$, where $|C_l|$ and $|C_k|$ are the number of images of C_l and C_k , respectively, x_l^i and x_k^j are the feature representations of images in C_l and C_k , respectively, $k(x_l^i, x_k^j) = c / \sqrt{|x_l^i - x_k^j|^2 + c}$ (c is a scalar). The average inter-concept visual similarity S_{int} of each two categories in D is defined as:

$$S_{int} = \frac{2}{|D|(|D| - 1)} \sum_{l=1}^{|D|} \sum_{k=l+1}^{|D|} s_{int}(C_l, C_k) \quad (7)$$

We use three kinds of hand-crafted features (i.e., Gist: used in [64], HOG: Histograms of Oriented Gradients [65], LBP: Local Binary Patterns [66].) to calculate C_{inn} and S_{int} , and set $c = 1.0$. These three kinds of features can depict the characteristics of the dataset on different aspects. As illustrated in Table 4, the trends of the statistical results on different datasets are almost the same in most cases, making the analysis be more comprehensive.

5.2 Evaluated Datasets and Settings

We construct some datasets of different image complexities, which include simple character images and images with different number of objects, e.g., general object images and scene images. In addition to the above images, facing vertical fields, we establish some fine-grained datasets (i.e., food and flower datasets). To guarantee that these datasets have the same dataset diversity, we refer to miniImagenet, and set the other datasets to have the same number of categories and the same number of samplers per category as miniImagenet. These datasets are detailedly described below. i) We collect and establish a handwritten character dataset, called **miniCharacter**, which is generated and annotated by 15 volunteers. MiniCharacter includes various characters such as english letters, numbers, mathematical symbols. The total number of categories is 84, and each of category has 100 images. The 64 and 20 categories are used as base and novel categories, respectively. ii) **MiniImagenet** [21] uses 64 and 20 categories as base and novel categories, respectively, where each category contains 600 images. iii) **MiniPlaces** is a subset of Places365 [6]. It uses 64 and 20 categories as base and novel categories, respectively, where each category contains 600 images. iv) **MiniFlower** is sampled from flower dataset [67] provided from 2018 FGVCxFlower Classification Challenge. It uses 64, 20 categories as base, novel categories, respectively, where each category contains 600 images. v) **MiniFood** is sampled from Food101 [68]. It uses 64 and 20 categories as base and novel categories, respectively, where each category contains 600 images. Experiments are conducted with four few-shot learning methods (i.e., PN, RN, MAML, adaCNN). Evaluating each model, we use the same architecture of few-shot learning methods, the same number of test tasks, and evaluation index as Section 4.

5.3 Analysis on Dataset Structure

This subsection aims to analyze performance differences on different datasets from their characteristics of dataset structures. Table 2 illustrates image complexity of evaluated datasets. It can be observed that the image complexity in miniCharacter is lowest. Each character image contains only one character with clear background. Besides, visual patterns of different kinds of characters are also very different. From Table 3, we can obtain that the FSIR performance on miniCharacter is significantly higher than that on the other datasets. From this special case of miniCharacter, we can find that image complexity plays an important role in FSIR. Character images are very different with natural images such as object, scene and food images. In the following, we mainly focus on comparisons and discussions on the other four datasets from characteristics of dataset structures.

As illustrated in Table 2, image complexity in miniFlower is the highest. However, the FSIR performance on miniFlower is not the lowest, which is higher than miniFood and comparable with miniImagenet and miniPlaces, as shown in Table 3. The reasons can be explained as follows. i) MinFlower is a special kind of fine-grained image dataset, where images in the same category are very similar. As shown in Fig. 10, although image complexity is very high with clustered edges and detailed component information, visual texture and structural patterns of images in the same

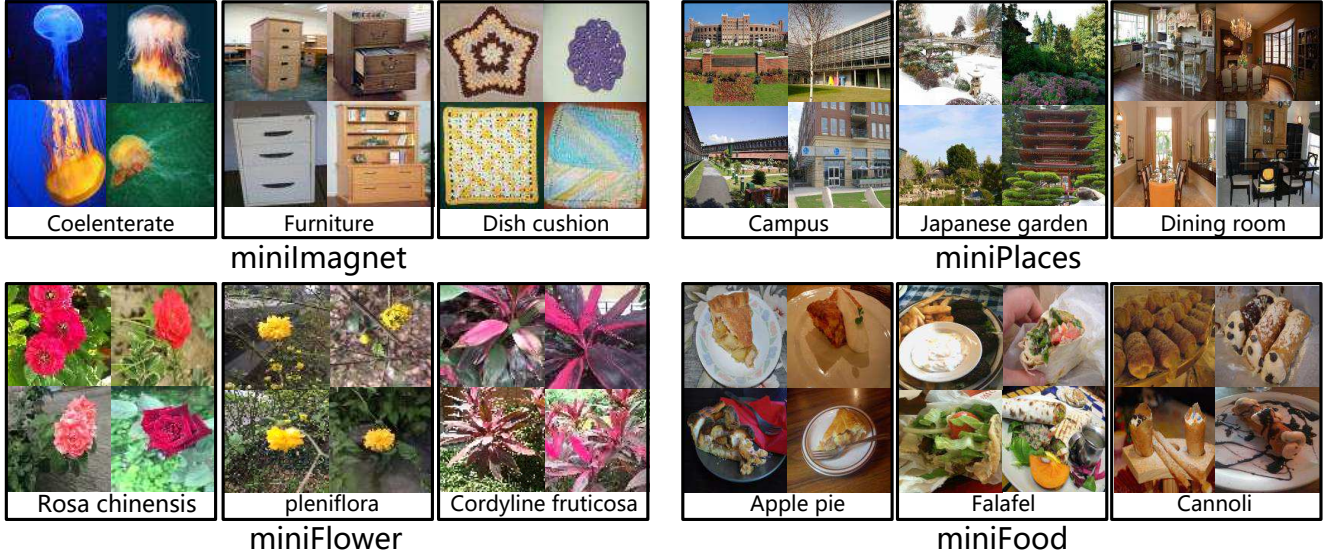


Fig. 10. Some image examples in different datasets

TABLE 2
The image complexity in different datasets.

Datasets	P_{EP}	E_{2D}
MiniCharacter	0.048	2.190
MiniImagenet	0.225	7.045
MiniPlaces	0.254	7.411
MiniFlower	0.325	8.012
MiniFood	0.259	7.407

TABLE 3
5-way 1-shot accuracy (%) on different datasets.

Datasets	PN	RN	MAML	adaCNN
MiniCharacter	86.17	91.83	85.45	83.91
MiniImagenet	49.42	51.38	48.70	48.26
MiniPlaces	49.00	50.62	48.49	50.05
MiniFlower	48.73	50.73	49.32	48.56
MiniFood	41.41	45.68	43.55	44.94

category are very similar. MiniFlower has the highest inner-concept visual consistency C_{inn} calculated with the three features, as illustrated in Table 4. This may lead to that the task of flower recognition is relatively easier, even for the case of FSIR. ii) As categories in miniFlower all belong to flower and they are close biological relatives, it is intuitive that visual patterns of different flower categories are also similar to some extent, as shown in Fig. 10. Thus base categories and novel categories in miniFlower present some relevance, which enables learned FSIR models to better recognize novel categories.

The FSIR performance on miniImagenet is higher than or comparable with the one on the other three datasets. The main reason is that image complexity in miniImagenet is lower than the one in the other datasets. However, the advantage of performance on miniImagenet is faint or not obvious when considering its image complexity is relatively lower than that of miniFlower. This phenomenon can be attributed to less relevance of base categories and novel categories in miniImagenet, which is reflected in following two aspects. i) Category labels in miniImageNet

TABLE 4
The average inner-concept visual consistency C_{inn} and inter-concept visual similarity S_{int} of novel categories in different datasets.

Datasets	C_{inn} (%)		S_{int} (%)		
	Gist	HOG	Gist	HOG	
MiniImagenet	36.84	17.50	30.94	35.10	16.85
MiniPlaces	36.19	18.90	30.03	34.14	18.07
MiniFlower	44.67	31.92	31.49	43.52	31.32
MiniFood	37.49	21.94	31.42	36.66	21.62

are sampled from a larger semantic space which brings greater diversities of semantic concepts, compared with miniFlower. This leads to less probabilities of sampling relevant base and novel categories in miniImagenet, when the number of base categories or novel categories are the same in all datasets (i.e., all datasets include 64 base categories and 20 novel categories). ii) Images in miniImagenet focus on single object, and different categories differ greatly in visual content, in contrast, different categories in miniFlower are similar, as shown in Fig. 10. Thus base categories and novel categories in miniImagenet present less relevance compared with miniFlower.

The FSIR performance from four methods on miniFood is the worst. The reasons can be explained as follows. i) As shown in Table 2, the image complexity of miniFood is much higher than the one of miniImagenet and miniPlaces. Besides, compared with the two datasets, the inter-concept visual similarity S_{int} of miniFood is higher, as shown in Table 4. Therefore, the performance on miniFood is worse than the one on miniImagenet and miniPlaces. ii) Although miniFlower and miniFood both belong to fine-grained datasets, there are fixed semantic patterns in miniFlower. For example, the flower consists of some semantic parts, such as petals and calyx. However, such semantic patterns do not exist in miniFood [69], and miniFood thus has a lower inner-concept visual consistency C_{inn} than miniFlower, as shown in Table 4. Therefore, the FSIR performance on miniFood is worse than the one on miniFlower.

5.4 Analysis on Few-shot Learning Methods

This subsection aims to analyze performance differences on different datasets from different few-shot learning methods. From Table 3, we observe that RN outperforms the other methods on all datasets. The possible reason is that RN uses a deeper architecture by employing two convolutional layers as a metric since the deeper architectures the better performances [11]. RN is a metric-based method with a parametric network as the metric, and PN is also a metric-based method but with a predefined metric. Metric-based methods recognize novel categories without task-specific adaptation, in contrast, meta-learning methods update the initial network such as weights in MAML, activations in adaCNN to recognize novel categories.

On the whole, compared with meta-learning methods, metric-based methods have advantages on datasets of low image complexities (e.g., miniCharacter, miniImagenet). However, these advantages become weak or even disadvantages on datasets of high image complexities (e.g., miniFlower, miniFood). A dataset of low image complexities is usually associated with a high inner-concept visual consistency or a low inter-concept visual similarity. On this dataset, metric-based methods without task-specific adaptation can still distinguish them, while meta-learning methods with the adaptation may introduce some noises. For example, two metric-based methods (i.e., PN, RN) both have better performances than two meta-learning methods (i.e., MAML, adaCNN) on miniCharacter. In contrast, a dataset of high image complexities is usually associated with a low inner-concept visual consistency or a high inter-concept visual similarity, and meta-learning methods can obtain further bonus with the adaptation to distinguish them. For example, two meta-learning methods both have better performances than PN on miniFood.

On miniPlaces, it can be observed that meta-learning methods obtain comparable performance with metric-based methods. Different scenes in miniPlaces usually contain object co-occurrences with different spatial layouts. Those co-occurrences may lead to inter-concept visual similarity, which may somewhat confuse metric-based methods. In contrast, meta-learning methods usually remain some shared weights, and adapt region-specific or task-specific weights with support set, those co-occurrences can somehow be learned by shared weights, making meta-learning methods be well adapted to miniPlaces.

When two meta-learning methods are compared on miniPlaces and miniFlower, it can be observed that adaCNN works better on scene-centric datasets miniPlace, in contrast, MAML obtains better performance on flower-centric datasets miniFlower. Scenes usually contain (object) region co-occurrences, which composite of different scenes with different spatial layout. With the “shared” regions, adaCNN can rapidly adapt activations to fit different spatial layouts, but MAML adjusts weights for adaptation which may broke the “shared” regions. Different categories of flowers usually contain similar spatial layouts (shapes), where the main differences appear in local detailed regions. AdaCNN may not capture these regions with adjustment on activations. In contrast, MAML has a bigger adaptive capacity by adjusting weights, which enables it to capture those detailed regions.

5.5 Discussion

Based on the above analysis, we can obtain:

- A dataset of a low image complexity is usually tested a high performance. Besides, inner-concept visual consistency and inter-concept visual similarity also can depict performance differences. For instance, since miniFlower has a higher inner-concept visual consistency, it has a better performance than miniFood, though miniFlower presents a higher image complexity.
- Metric-based methods may excel at recognizing novel categories of low image complexities, and meta-learning methods are promising solutions to handle novel categories of high ones.
- It's more effective to design FSIR architectures according to the characteristics of data distribution. For instance, MAML jointly update weights for task-specific adaptation, which is more suitable to fine-grained categories, such as miniFlower.

6 CONCLUSIONS

Few-shot image recognition (FSIR) is a significant research problem in the machine learning and computer vision community. In this paper, we study FSIR with dataset bias systematically. First, we investigate impact of transferable capabilities learned from distributions of base categories. We introduce instance diversity and category diversity to depict distributions of base categories, and relevance to describe relationships of base and novel categories. Experimental results on different sub-datasets of ImagNet demonstrate the relevance and two diversities can depict the transferable bias from distributions of base categories. Second, we investigate differences in performance on different datasets from characteristics of dataset structures and different few-shot learning methods. We introduce image complexity, inner-concept visual consistency, and inter-concept visual similarity to quantify characteristics of dataset structures. We conduct experiments on five datasets with four few-shot learning methods. Experimental analysis shows that the three quantifications can depict performance differences on different datasets and some insightful observations are obtained from the perspective of few-shot learning methods. We hope that some insight observations are helpful to guide future FSIR research.

REFERENCES

- [1] K. He, X. Zhang, S. Ren, and J. Sun, “Deep residual learning for image recognition,” in *Computer Vision and Pattern Recognition*, 2016, pp. 770–778.
- [2] C. Szegedy, S. Ioffe, V. Vanhoucke, and A. A. Alemi, “Inception-v4, inception-resnet and the impact of residual connections on learning,” in *Association for the Advancement of Artificial Intelligence*, 2017, pp. 4278–4284.
- [3] G. Huang, Z. Liu, L. van der Maaten, and K. Q. Weinberger, “Densely connected convolutional networks,” in *Computer Vision and Pattern Recognition*, 2017, pp. 2261–2269.
- [4] Y. LeCun, Y. Bengio, and G. Hinton, “Deep learning,” *Nature*, vol. 521, no. 7553, pp. 436–444, 2015.
- [5] J. Deng, W. Dong, R. Socher, L.-J. Li, K. Li, and L. Fei-Fei, “Imagenet: A large-scale hierarchical image database,” in *Computer Vision and Pattern Recognition*, 2009, pp. 248–255.

[6] B. Zhou, A. Lapedriza, A. Khosla, A. Oliva, and A. Torralba, "Places: A 10 million image database for scene recognition," *IEEE Transactions on Pattern Analysis and Machine Intelligence*, vol. 40, no. 6, pp. 1452–1464, 2018.

[7] S. Thrun and L. Pratt, "Learning to learn: introduction and overview," *Learning to learn*, pp. 3–17, 1998.

[8] H. F. Harlow, "The formation of learning sets." *Psychological Review*, vol. 56, no. 1, pp. 51–65, 1949.

[9] J. Snell, K. Swersky, and R. Zemel, "Prototypical networks for few-shot learning," in *Neural Information Processing Systems*, 2017, pp. 4080–4090.

[10] F. Sung, Y. Yang, L. Zhang, T. Xiang, P. H. Torr, and T. M. Hospedales, "Learning to compare: Relation network for few-shot learning," in *Computer Vision and Pattern Recognition*, 2018, pp. 1199–1208.

[11] W.-Y. Chen, Y.-C. Liu, Z. Kira, Y.-C. F. Wang, and J.-B. Huang, "A closer look at few-shot classification," in *International Conference on Learning Representations*, 2019.

[12] K. Lee, S. Maji, A. Ravichandran, and S. Soatto, "Meta-learning with differentiable convex optimization," in *Computer Vision and Pattern Recognition*, 2019, pp. 10 657–10 665.

[13] C. Finn, P. Abbeel, and S. Levine, "Model-agnostic meta-learning for fast adaptation of deep networks," in *International Conference on Machine Learning*, 2017, pp. 1126–1135.

[14] T. Munkhdalai, X. Yuan, S. Mehri, and A. Trischler, "Rapid adaptation with conditionally shifted neurons," in *International Conference on Machine Learning*, 2018, pp. 3661–3670.

[15] G. S. Dhillon, P. Chaudhari, A. Ravichandran, and S. Soatto, "A baseline for few-shot image classification," in *International Conference on Learning Representations*, 2020.

[16] O. Russakovsky, J. Deng, H. Su, J. Krause, S. Satheesh, S. Ma, Z. Huang, A. Karpathy, A. Khosla, M. Bernstein *et al.*, "Imagenet large scale visual recognition challenge," *International journal of computer vision*, vol. 115, no. 3, pp. 211–252, 2015.

[17] L. Fei-Fei, R. Fergus, and P. Perona, "One-shot learning of object categories," *IEEE Transactions on Pattern Analysis and Machine Intelligence*, vol. 28, no. 4, pp. 594–611, 2006.

[18] B. M. Lake, R. Salakhutdinov, and J. B. Tenenbaum, "Human-level concept learning through probabilistic program induction." *Science*, vol. 350, no. 6266, pp. 1332–1338, 2015.

[19] A. Santoro, S. Bartunov, M. Botvinick, D. Wierstra, and T. Lillicrap, "Meta-learning with memory-augmented neural networks," in *International Conference on Machine Learning*, 2016, pp. 1842–1850.

[20] G. Koch, R. Zemel, and R. Salakhutdinov, "Siamese neural networks for one-shot image recognition," in *ICML Deep Learning Workshop*, vol. 2, 2015.

[21] O. Vinyals, C. Blundell, T. Lillicrap, D. Wierstra *et al.*, "Matching networks for one shot learning," in *Neural Information Processing Systems*, 2016, pp. 3630–3638.

[22] J. Schmidhuber, "Evolutionary principles in self-referential learning, or on learning how to learn: the meta-meta... hook," Ph.D. dissertation, Technische Universität München, 1987.

[23] D. Naik and R. Mammone, "Meta-neural networks that learn by learning," in *IJCNN International Joint Conference on Neural Networks*, vol. 1, 1992, pp. 437–442.

[24] T. Munkhdalai and H. Yu, "Meta networks," in *International Conference on Machine Learning*, 2017, pp. 2554–2563.

[25] M. Dixit, R. Kwitt, M. Niethammer, and N. Vasconcelos, "Aga: Attribute-guided augmentation," in *Computer Vision and Pattern Recognition*, 2017, pp. 3328–3336.

[26] Z. Chen, Y. Fu, Y. Zhang, Y.-G. Jiang, X. Xue, and L. Sigal, "Semantic feature augmentation in few-shot learning," *arXiv preprint arXiv:1804.05298*, 2018.

[27] B. Hariharan and R. Girshick, "Low-shot visual recognition by shrinking and hallucinating features," in *International Conference on Computer Vision*, 2017, pp. 3018–3027.

[28] E. Schwartz, L. Karlinsky, J. Shtok, S. Harary, M. Marder, A. Kumar, R. Feris, R. Giryes, and A. Bronstein, "Delta-encoder: an effective sample synthesis method for few-shot object recognition," in *Neural Information Processing Systems*, 2018, pp. 2850–2860.

[29] S. Gidaris, A. Bursuc, N. Komodakis, P. P. Perez, and M. Cord, "Boosting few-shot visual learning with self-supervision," in *International Conference on Computer Vision*, 2019, pp. 8058–8067.

[30] X. Li, Q. Sun, Y. Liu, Q. Zhou, S. Zheng, T.-S. Chua, and B. Schiele, "Learning to self-train for semi-supervised few-shot classification," in *Neural Information Processing Systems*, 2019, pp. 10 276–10 286.

[31] M. Ren, S. Ravi, E. Triantafillou, J. Snell, K. Swersky, J. B. Tenenbaum, H. Larochelle, and R. S. Zemel, "Meta-learning for semi-supervised few-shot classification," in *International Conference on Learning Representations*, 2018.

[32] Y. Liu, J. Lee, M. Park, S. Kim, E. Yang, S. J. Hwang, and Y. Yang, "Learning to propagate labels: Transductive propagation network for few-shot learning," in *International Conference on Learning Representations*, 2019.

[33] Z. Yu, L. Chen, Z. Cheng, and J. Luo, "Transmatch: A transfer-learning scheme for semi-supervised few-shot learning," in *Computer Vision and Pattern Recognition*, 2020, pp. 12 856–12 864.

[34] O. Sbai, C. Couprie, and M. Aubry, "Impact of base dataset design on few-shot image classification," *arXiv preprint arXiv:2007.08872*, 2020.

[35] G. French, M. Mackiewicz, and M. Fisher, "Self-ensembling for visual domain adaptation," in *International Conference on Learning Representations*, 2018.

[36] W. Zellinger, T. Grubinger, E. Lughofe, T. Natschläger, and S. Saminger-Platz, "Central moment discrepancy (cmd) for domain-invariant representation learning," in *International Conference on Learning Representations*, 2017.

[37] Y. Ganin and V. Lempitsky, "Unsupervised domain adaptation by backpropagation," in *International Conference on Machine Learning*, 2015, pp. 1180–1189.

[38] M. Long, Y. Cao, J. Wang, and M. I. Jordan, "Learning transferable features with deep adaptation networks," in *International Conference on Machine Learning*, 2015, pp. 97–105.

[39] X. Li, L. Herranz, and S. Jiang, "Multifaceted analysis of fine-tuning in deep model for visual recognition," *arXiv preprint arXiv:1907.05099*, 2019.

[40] H. Azizpour, A. S. Razavian, J. Sullivan, A. Maki, and S. Carlsson, "Factors of transferability for a generic convnet representation," *IEEE Transactions on Pattern Analysis and Machine Intelligence*, vol. 38, no. 9, pp. 1790–1802, 2016.

[41] M. Long, H. Zhu, J. Wang, and M. I. Jordan, "Unsupervised domain adaptation with residual transfer networks," in *Neural Information Processing Systems*, 2016, pp. 136–144.

[42] E. Tzeng, J. Hoffman, K. Saenko, and T. Darrell, "Adversarial discriminative domain adaptation," in *Computer Vision and Pattern Recognition*, 2017, pp. 2962–2971.

[43] J.-Y. Zhu, T. Park, P. Isola, and A. A. Efros, "Unpaired image-to-image translation using cycle-consistent adversarial networks," in *International Conference on Computer Vision*, 2017, pp. 2223–2232.

[44] J. Hoffman, E. Tzeng, T. Park, J.-Y. Zhu, P. Isola, K. Saenko, A. A. Efros, and T. Darrell, "Cycada: Cycle-consistent adversarial domain adaptation," in *International Conference on Machine Learning*, 2018, pp. 1989–1998.

[45] Y. Zhang, H. Tang, K. Jia, and M. Tan, "Domain-symmetric networks for adversarial domain adaptation," in *Computer Vision and Pattern Recognition*, 2019, pp. 5031–5040.

[46] S. Cui, S. Wang, J. Zhuo, C. Su, Q. Huang, and Q. Tian, "Gradually vanishing bridge for adversarial domain adaptation," in *Computer Vision and Pattern Recognition*, 2020, pp. 12 455–12 464.

[47] M. Mancini, S. R. Bulo, B. Caputo, and E. Ricci, "Adagraph: Unifying predictive and continuous domain adaptation through graphs," in *Computer Vision and Pattern Recognition*, 2019, pp. 6561–6570.

[48] S. Motiian, Q. Jones, S. M. Iranmanesh, and G. Doretto, "Few-shot adversarial domain adaptation," in *Neural Information Processing Systems*, 2017, pp. 6670–6680.

[49] B. Kang and J. Feng, "Transferable meta learning across domains," in *Uncertainty in Artificial Intelligence*, 2018, pp. 177–187.

[50] P. Welinder, S. Branson, T. Mita, C. Wah, F. Schroff, S. Belongie, and P. Perona, "Caltech-ucsd birds 200," 2010.

[51] H.-Y. Tseng, H.-Y. Lee, J.-B. Huang, and M.-H. Yang, "Cross-domain few-shot classification via learned feature-wise transformation," in *International Conference on Learning Representations*, 2020.

[52] Y. Guo, N. C. F. Codella, L. Karlinsky, J. R. Smith, T. Rosing, and R. Feris, "A new benchmark for evaluation of cross-domain few-shot learning," *arXiv preprint arXiv:1912.07200*, 2019.

[53] R. Vuorio, S.-H. Sun, H. Hu, and J. J. Lim, "Multimodal model-agnostic meta-learning via task-aware modulation," in *Neural Information Processing Systems*, 2019, pp. 1–12.

[54] H. Yao, Y. Wei, J. Huang, and Z. Li, "Hierarchically structured meta-learning," in *International Conference on Machine Learning*, 2019, pp. 7045–7054.

- [55] E. Triantafillou, T. Zhu, V. Dumoulin, P. Lamblin, U. Evci, K. X. ad Ross Goroshin, K. S. Carles Gelad and, P.-A. Manzagol, and H. Larochelle, "Meta-dataset: A dataset of datasets for learning to learn from few examples," in *International Conference on Learning Representations*, 2020.
- [56] S. Thrun and L. Pratt, *Learning to learn*. Springer Science & Business Media, 2012.
- [57] G. A. Miller, "Wordnet: a lexical database for english," *Communications of the ACM*, vol. 38, no. 11, pp. 39–41, 1995.
- [58] J. Yosinski, J. Clune, Y. Bengio, and H. Lipson, "How transferable are features in deep neural networks?" in *Neural Information Processing Systems*, 2014, pp. 3320–3328.
- [59] T. Cao, M. T. Law, and S. Fidler, "A theoretical analysis of the number of shots in few-shot learning," in *International Conference on Learning Representations*, 2020.
- [60] X.-S. Wei, P. Wang, L. Liu, C. Shen, and J. Wu, "Piecewise classifier mappings: Learning fine-grained learners for novel categories with few examples," *IEEE Transactions on Image Processing*, vol. 28, no. 12, pp. 6116–6125, 2019.
- [61] J. Fan, X. He, N. Zhou, J. Peng, and R. Jain, "Quantitative characterization of semantic gaps for learning complexity estimation and inference model selection," *IEEE Transactions on Multimedia*, vol. 14, no. 5, pp. 1414–1428, 2012.
- [62] J. Canny, "A computational approach to edge detection," *IEEE Transactions on Pattern Analysis and Machine Intelligence*, no. 6, pp. 679–698, 1986.
- [63] K. G. Larkin, "Reflections on shannon information: In search of a natural information-entropy for images," *arXiv preprint arXiv:1609.01117*, 2016.
- [64] A. Oliva and A. Torralba, "Modeling the shape of the scene: A holistic representation of the spatial envelope," *International Journal of Computer Vision*, vol. 42, no. 3, pp. 145–175, 2001.
- [65] N. Dalal and B. Triggs, "Histograms of oriented gradients for human detection," in *Computer Vision and Pattern Recognition*, 2005, pp. 886–893.
- [66] T. Ojala, M. Pietikainen, and T. Maenpaa, "Multiresolution gray-scale and rotation invariant texture classification with local binary patterns," *IEEE Transactions on Pattern Analysis and Machine Intelligence*, vol. 24, no. 7, pp. 971–987, 2002.
- [67] "Fgvc flowers dataset." [Online]. Available: <https://sites.google.com/view/fgvc5/competitions/fgvcx/flowers>
- [68] L. Bossard, M. Guillaumin, and L. J. V. Gool, "Food-101 še mining discriminative components with random forests," *European Conference on Computer Vision*, vol. 8694, pp. 446–461, 2014.
- [69] W. Min, S. Jiang, L. Liu, Y. Rui, and R. Jain, "A survey on food computing," *ACM Computing Surveys*, vol. 52, no. 5, p. 92, 2019.